High acetone soluble organosolv lignin extraction and its application towards green antifouling and wear-resistant coating

International Journal of Biological Macromolecules 282 (2024) 137456

Contents lists available at ScienceDirect

International Journal of Biological Macromolecules

journal homepage: www.elsevier.com/locate/ijbiomac

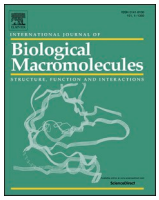

High acetone soluble organosolv lignin extraction and its application towards green antifouling and wear-resistant coating

Zhipeng Wu [a], Petter Paulsen Thoresen [b], Dominik Maršík [c], Leonidas Matsakas [b], Markéta Kulišová [c], Karel Fous [c], Olga Maťátková [c], Jan Masák [c], Ulrika Rova [b], Erik Ytreberg [d], Lena Granhag [d], Paul Christakopoulos [b,*], Yijun Shi [a,*]

[a] Division of Machine Elements, Luleå University of Technology, 97187 Luleå, Sweden
[b] Biochemical Process Engineering, Division of Chemical Engineering, Department of Civil, Environmental and Natural Resources Engineering, Luleå University of Technology, 97187 Luleå, Sweden
[c] Department of Biotechnology, University of Chemistry and Technology, 166 28 Prague, Czech Republic
[d] Department of Mechanics and Maritime Sciences, Chalmers University of Technology, SE 412 96, Gothenburg, Sweden

ARTICLE INFO

Keywords:
Lignin
Polyurethane
Coating
Antifouling

ABSTRACT

Marine fouling poses significant challenges to the efficiency and longevity of marine engineering equipment. To address this issue, developing effective marine antifouling coatings is critical to ensure the economic viability, environmental sustainability, and safety of offshore operations. In this study, we developed an innovative green antifouling and wear-resistant coating based on lignin, a renewable and sustainable resource. Lignin is considered environmentally friendly because it is abundant, biodegradable, and reduces reliance on petroleum-based materials. The coating was formulated with a controlled hydrophilic-to-hydrophobic ratio of 2:8, leveraging lignin's unique properties. Applying lignin increased the water contact angle by 14.5 %, improving surface hydrophobicity and contributing to the coating's antifouling efficacy. Moreover, the mechanical strength of the coating was enhanced by approximately 200 %, significantly boosting its durability in harsh marine environments. Additionally, the friction coefficient was reduced by about 85 %, further preventing organism adhesion. These results demonstrate that lignin-based coatings offer a greener alternative to traditional antifouling solutions. The results of this study not only help advance antifouling coating technology but are also consistent with the broader goal of promoting environmental responsibility in marine engineering practice.

1. Introduction

Marine engineering equipment and offshore structures face major challenges from corrosion and biofouling [1]. Marine fouling, characterized by the adhesion of unwanted organisms to submerged surfaces, remains a persistent challenge with far-reaching consequences for the efficiency and durability of maritime structures [2]. With the continuous development of the marine industry and economy, the economic losses caused by marine fouling organisms are increasing. Therefore, effective and economical prevention methods are receiving increasing attention. Marine antifouling coatings are integral to the maritime industry and offer numerous advantages over traditional antifouling methods [3]. Traditional marine antifouling coatings play a vital role in preventing the accumulation of marine life on underwater surfaces and are, therefore, of huge interest to the maritime industry. These coatings significantly improve operational efficiency by reducing hull drag, resulting in improved fuel efficiency and significant cost savings for ship operators and reducing the environmental impact of the shipping sector. Additionally, they play a key role in extending the service life of marine structures and preventing corrosion and deterioration caused by fouling organisms. An additional environmental impact of those coatings that is worth mentioning is that they help prevent the spread of invasive species, while they also aid regulatory compliance with international maritime standards [4]. These coatings also keep the hull clean and free of dirt, improving safety and reducing the risk of accidents and collisions [5]. Overall, conventional marine antifouling coatings are integral in ensuring the economic viability, environmental sustainability, and safety of offshore operations.

Traditional antifouling coatings' environmental impact puts a considerable shade on their efficacy. As these paints include germ-

* Corresponding authors.
E-mail addresses: paul.christakopoulos@ltu.se (P. Christakopoulos), yijun.shi@ltu.se (Y. Shi).

https://doi.org/10.1016/j.ijbiomac.2024.137456
Received 25 June 2024; Received in revised form 31 October 2024; Accepted 7 November 2024
Available online 12 November 2024

killing substances like sliver [6], copper [7] and tributyltin [8], there are valid worries regarding their influence on marine environments. In addition, petroleum-based materials such as silicone-based polymers, polyurethane, and epoxy resins are widely used in commercial coatings [9]. The continual discharge of such chemicals into the aquatic environment has raised environmental awareness and forced tighter restrictions, highlighting the importance of less damaging coatings to aquatic life [10]. Furthermore, long-term use of some chemicals has resulted in a disturbing development: the formation of drug resistance in some fouling species [11]. Despite long-term exposure to antifouling methods, robust organisms persist, reducing their overall efficiency. This adaptive reaction not only weakens the coating's intended protective role but also underscores the critical need for alternatives to avoid the difficulties associated with resistance development.

One potential green solution may be lignin, a fascinating natural polymer present in plant cell walls [12]. Lignin reveals a dual nature beyond its usual role as a structural component in plant tissues, exposing itself as a strong antibacterial agent [13]. Because of this distinguishing feature, lignin has strong potentials for creating ecologically responsible anti-fouling coatings [14]. During production, lignin, a renewable resource, reduces reliance on petroleum-based materials, lowering the carbon footprint [15]. Lignin provides a possible alternative to established biocidal techniques by utilizing its intrinsic antibacterial characteristics. Lignin could not only protect submerged buildings by increasing their lifetime and operating efficiency, but also contribute to achieving larger environmental aims [16]. Some researchers have focused on the lignin-based coating. Di Wang et al. studied the development of organosolv lignin-based polyurethane (OS-lignin-PU) coatings [17]. Their optimized lignin-PU coating demonstrated higher hardness, reduced maximum scratch depth, and a lower friction coefficient compared to coatings with less lignin content. These enhanced properties make it suitable for use as both a corrosion protection coating and an anti-wear coating. Lignin coatings offer significant environmental benefits compared to traditional coatings. The use of lignin in coatings minimizes the release of toxic biocides into marine environments, mitigating harm to aquatic life. The investigation of lignin-based coatings represents a paradigm change toward environmentally responsible nautical activities, symbolizing the possibility for a cleaner, more sustainable future.

In this study, we propose an innovative marine antifouling coating, which utilizes lignin as an environmentally friendly raw material, aiming to improve the antibacterial and antifouling properties of the coating performance while contributing to reducing the environmental impact associated with traditional antifouling coatings. This study aims to explore the application potential of lignin-based coatings in marine engineering, particularly its effectiveness in preventing biological adhesion and improving wear resistance. In addition, by systematically evaluating the performance of coatings with different lignin sources (organosolv lignin isolated from beech and spruce sawdust) and different processing conditions (with/without H_2SO_4), this article aims to provide a theoretical foundation and practical guidance for the development of a new generation of environmentally friendly and efficient marine antifouling coatings from lignin. Furthermore, the byproducts generated during lignin extraction, such as residual lignin, cellulose, and hemicellulose, can be utilized for bio-based materials, biofuels, or chemical feedstocks, enhancing sustainability and supporting a circular bioeconomy. The results of this research are not only expected to promote the development of environmentally friendly marine anti-fouling technology but also provide a novel strategy for the sustainable use of marine engineering materials.

2. Materials and methods

2.1. Raw materials

Beech sawdust (LIGNOCEL HBS 150/500; Rettenmaier Sweden KB JRS), Spruce sawdust (obtained from a local mill in northern Sweden), sulfuric acid (H_2SO_4; 95.0–98.0 %; Sigma-Aldrich), ethanol (absolute, VWR), Polydimethylsiloxane (PDMS) (Mn ≈ 4000 g/mol; Shanghai Tiger Polymer Technology Co., Ltd., China), Isophorone diisocyanate (IPDI; 98 %; mixture of isomers; Sigma-Aldrich), Poly(ethylene glycol) (PEG-400; average Mn 400; Sigma-Aldrich), Poly(ethylene glycol) (PEG-2000; average Mn 2000; Sigma-Aldrich), acetone (VWR) were used in this study. Commercial coating for comparison: MILLIE NCT and ECO POWER RACING from Hempel. Unless otherwise stated, all reagents were used as received without further purification.

2.2. Lignin isolation

Organosolv lignin was isolated from beech sawdust (B and BA for lignin extracted without or with acid catalyst) and spruce sawdust (denoted as S and SA for lignin extracted without or with acid catalyst). In short, the lignocellulosic material was processed in an air-heated multidigester system (Haato, Vantaa, Finland) in 60/40 vol% ethanol/water at 180 °C and for 60 min for beech and 50/50 vol% at 200 °C for 30 min for spruce. In both materials, the solid-to-liquid ratio was set at 1/10 g/mL and 1 wt% H_2SO_4 (on a dry biomass basis) was used as the acid catalyst (when applicable). After the organosolv treatment, the generated slurry was vacuum filtered and the liquid fraction, containing the dissolved lignin and sugars mainly from hemicellulose, was processed by evaporation in a rotary evaporator (Heidolph, Schwabach, Germany) to recover ethanol and in turn reduce the solubility of lignin. Thereafter, lignin was recovered by centrifugation at 10,000 xg for 15 min at 4 °C (5804R; Eppendorf, Hamburg, Germany) and freeze-dried (Lyoquest; Telstar, Terrassa, Spain) before being stored in plastic flasks in room temperature. The extraction yield of the applied lignin was about 86 %.

2.3. Quantitative ^{31}P NMR analysis of lignin

A procedure similar to that previously reported was applied [18–20]. In short, approx. 30 mg of lignin was added to 425 μL of pyridine/CDCl3 (1.6:1). 100 μL of the standard solution, prepared using N-hydroxy-5-norbornene-2,3-dicarboxylic acid imide (e-HNDI) or cholesterol at a concentration of approx. 0.1 M in the previously mentioned solvent mixture (pyridine/$CDCl_3$) with 50 mg/mL of Cr(III) acetylacetonate (relaxating agent) and 75 μL of 2-chloro-4,4,5,5-tetramethyl-1,3,2-dioxaphospholane (Cl-TMPD). After 1 h of mixing at room temperature, the functionalized solution was transferred to an NMR tube (5 mm). ^{31}P NMR spectra were recorded on a Bruker AVANCE III 400 MHz spectrometer equipped with a BBI probe and an inverse-gated decoupling technique with a probe temperature of 20 °C. NMR data were processed with MestreNova (Version 8.1.1, Mestrelab Research).

2.3.1. Synthesis of the hydration part of the coating

PEG-400 (10 g) was added to a three-necked flask equipped with an electric stirrer (RW 20 digital; Germany) and a thermocouple thermometer. It was heated to 75 °C, and IPDI (11.12 g) was carefully added to the flask. The mixture was stirred and reacted at 75 °C for 1 h, and thereafter acetone (282.61 g) was added to dilute the mixture. The solution was further cooled down room temperature. PDMS-4000 (100 g) was introduced into the mixture slowly. This final solution was left at room temperature under mixing for another 12 h to complete the reaction, resulting to an acetone solution containing the hydration layer (PMDS-PU) at a content of 30 wt% (Fig. 1).

2.3.2. Synthesis of the hydrophobic part of the coating

PEG-2000 (50 g) was heated at 75 °C for 0.5 h in a three-necked flask fitted with an electric stirrer (RW 20 digital; Germany), and a thermocouple thermometer. Then, IPDI (11.12 g) was carefully added to the flask. The mixture was mixed and reacted at 75 °C for 1 h. Thereafter, PEG-400 (10 g) was slowly added to the mixture and left to react for 1.5

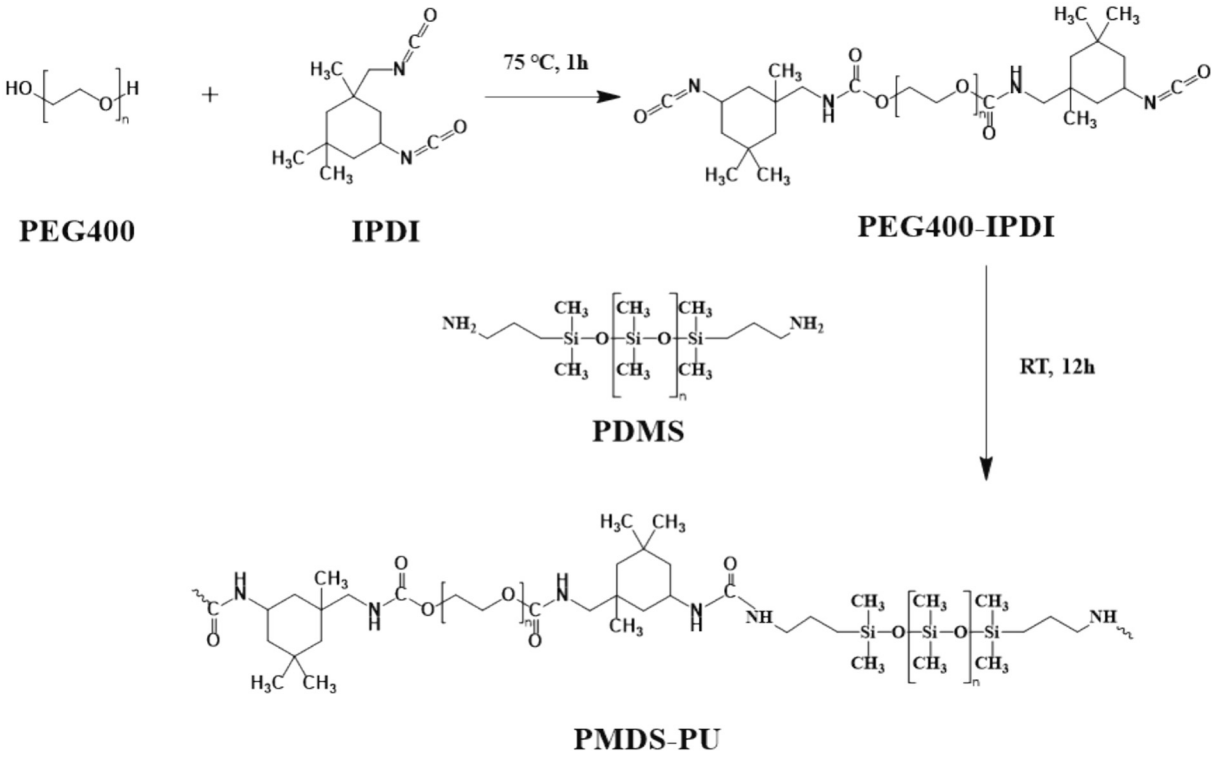

Fig. 1. Synthetic route of PDMS-PU.

h. The heating was then turned off, and acetone (165.94 g) was added to achieve a final content of 70 wt%, and the temperature gradually lowered to room temperature. This addition was followed by a complete reaction period of 12 h at room temperature. Resulting in an acetone solution containing 30 wt% of the hydrophilic layer PEG-PU; Fig. 2).

2.3.3. Preparation of the anti-fouling coating solution

To prepare the coating solution, hydrophilic and hydrophobic PUs were mixed in a mass ratio of 2:8 to obtain a basic coating solution. The solution was then supplemented with lignin by the proportions specified in Table 1.

2.3.4. Final coating preparation

Stainless steel coupons (DC01, 13 mm diameter, 2 mm thickness) were coated with a 10 % (w/w) concentration of coatings, which were previously diluted with acetone. The application process involved three layers of coating applied uniformly using a 0.4 mm airbrush (Colani, Harder & Steenbeck, DE). The airbrush was positioned at 5–7 cm, and an air pressure of 2.5 bar was maintained. Following coating, the coupons were left to dry under UV radiation ($\lambda = 254$ nm) exposure for 30 min on each side to sterilize the surfaces. Subsequently, the coupons were aseptically transferred to 24-well microtiter plates (TPP, CH), underwent a sterile distilled water wash twice for 20 min, and were left to dry. Coating coverage was assessed using scanning electron microscopy

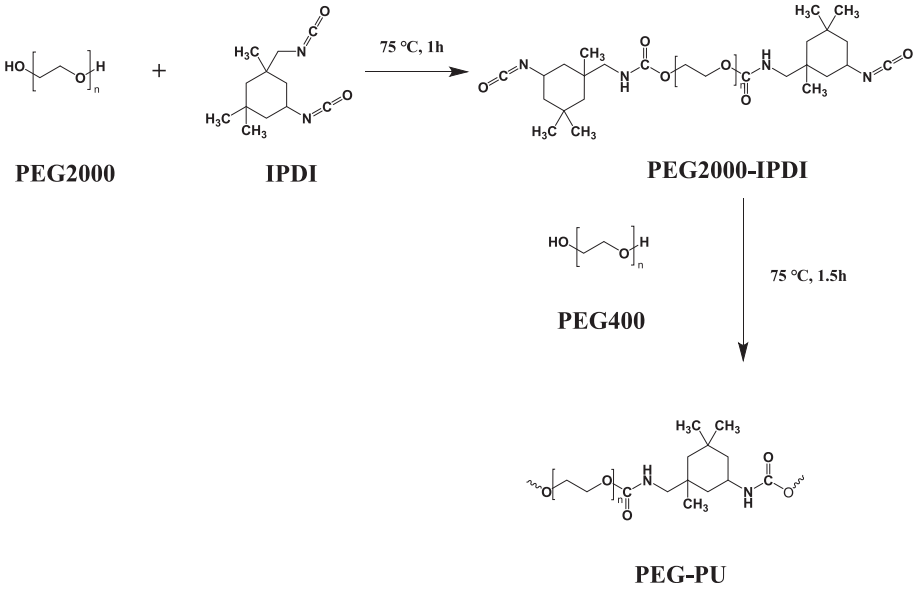

Fig. 2. Synthetic route of PEG-PU.

Table 1
Ratios of the lignin antifouling coating solution with a solid content of 10 % (*w*/w).

	0 % Lignin-PU	10 % BA-PU	20 % BA-PU	30 % BA-PU	40 % BA-PU	10 % SA-PU	20 % SA-PU	30 % SA-PU	40 % SA-PU
BA/g	0	0.1	0.2	0.3	0.4	0	0	0	0
SA/g	0	0	0	0	0	0.1	0.2	0.3	0.4
Hydrophilic PU/g	0.2	0.18	0.16	0.14	0.12	0.18	0.16	0.14	0.12
Hydrophobic PU/g	0.8	0.72	0.64	0.56	0.48	0.72	0.64	0.56	0.48
Acetone /g	9	9	9	9	9	9	9	9	9

Note: 10 % BA-PU refers to an antifouling coating containing 10 % mass fraction of BA lignin.

(SEM) with energy-dispersive X-ray spectroscopy (EDS). Commercial coatings "Commercial 1" (biocide-free mixture of petroleum and organic substances) and "Commercial 2" (active ingredient Cu_2O) were applied to the steel coupon under identical conditions as the lignin coatings, with the number of layers applied following the manufacturer's recommendations.

2.4. Characterization of the coatings

2.4.1. Fourier transform infrared spectroscopy

The Fourier transform infrared - Attenuated total reflectance (FTIR-ATR) spectra were recorded using a Nicolet™ Summit™ FTIR spectrometer. The number of scans is 16, and the resolution is 4 cm^{-1}. The wave number range was determined to be 4000–400 cm^{-1} This technique was performed to investigate the chemical interactions and bonding between lignin and polyurethane. It allows us to confirm the successful formation of hydrogen bonds and other molecular interactions within the composite coating.

2.4.2. Thermogravimetric analysis

Thermogravimetric analysis (TGA) and differential scanning calorimetry (DSC) was conducted to assess decomposition profile and the thermal stability of the coatings. The lignin and Lignin-PU samples were dried at 105 °C prior to TGA and DSC. TGA was carried out using a TGA 8000-PerkinElmer, USA, with an integrated thermal analyser, nitrogen flow rate (100 mL/min), heating rate (10 °C/min), and a test temperature range from room temperature to 800 °C. DSC was performed using the DSC 3+ thermal analysis system (METTLER TOLEDO), where a 5–10 mg sample was placed on an aluminium pan and heated at a rate of 10 °C/min under a nitrogen flow in a heat/cool/heat cycle from −50 to 210 °C. The glass transition temperatures (Tg) were calculated using the second cycle.

2.4.3. Water contact angle test

Water contact angle measurements were performed using an Attention Theta optical tensiometer (Biolin Scientific) at 20 °C. This test was performed to assess the hydrophobicity of the coatings. A 4 μL distilled water droplet was used for each measurement. The reported values are the average value of at least 3 measurements ± standard deviation.

2.4.4. Nano scratch and Nano indent test

Nano scratch testing was performed using a 90° conical indenter with a diameter of 50 um. The load was 1 mN, the scanning speed was 5 μm/s, and the scanning length was 500 μm. This test was used to evaluate the mechanical strength and scratch resistance of the coatings.

2.4.5. Bovine serum albumin absorption

Quartz crystal microbalance with dissipation monitoring (QCM-D) test using BSA was carried out to measure protein adsorption on the coating surface, as protein accumulation is a precursor to biofouling. Lower protein adsorption indicates better antifouling properties. The QCM-D investigated protein surface adsorption utilizing the Q-Sense AB equipment and bovine serum albumin (BSA) as a model protein. At the nanogram level, QCM-D can monitor adsorption-desorption events on the sensor surface in real time. First, the sensor was ultrasonically cleaned with acetone for 5 min before blowing it clean and dry with compressed air. Then, a dilute solution (each coating tested was dissolved in acetone to form a dilute solution, 0.1 % wt%) of the tested sample was added drop by drop onto the sensor. The sensor was then dried in an oven at 50 °C for 3 h. The coated sensor was mounted in the flow cell, where initially pure deionized water passed through the chamber at room temperature at a flow rate of 100 μL/min until all frequency overtones were stabilized. Subsequently, a 1 g L^{-1} BSA solution passed through at the same flow rate until the saturation point was observed and stabilized. Finally, the solution was switched back to deionized water to observe any frequency changes.

2.4.6. Scanning electron microscopy with energy-dispersive X-ray spectroscopy

The coatings coverages were characterized using a scanning electron microscope MIRA 3 (FE-SEM, Tescan, Brno, Czech Republic) with a perpendicular in-beam secondary electron detector at high magnifications at 1000 x and accelerating voltages of 30 kV (Schottky emitter). The chemical analysis of coating was carried out using the Quantax 200 energy-dispersive X-ray spectrometer with Bruker's XFlash 6 detector (Bruker Nano GmbH, Berlin, Germany).

The chemical analysis of coatings was carried out using the SEM-equipped Quantax 200 energy-dispersive X-ray spectrometer with the Bruker's XFlash 6 detector with magnification 1000 x, accelerating voltage of 30 kV, interaction depth of around 9.1 μm and interaction radius 5.1 μm.

2.5. Anti-bacterial testing

2.5.1. Microorganism, growth media and conditions

A colony of cells was transferred from solid medium to liquid Marine Broth 2216 (Millipore, USA) or Luria Bertani (LB) medium (10 g L^{-1} tryptone, 10 g L^{-1} NaCl, 5 g L^{-1} yeast extract), depending on the microorganism (Table 2). Cultivation occurred for 24 h at 150 rpm and the optimal temperature for the specific microorganism. After cultivation, cells were separated by centrifugation (10 min; 10 °C; 9000 ×g). The resulting pellet was resuspended in fresh Marine Broth/LB medium to achieve $OD_{600} = 0.600 \pm 0.012$. A 2.5 mL cell suspension was then transferred to polystyrene 24-well microtiter plates containing coated coupons. Afterwards, the coupons were incubated for 24 h at 150 rpm at the temperature suitable for the respective bacterial strain. Following incubation, the suspension was discarded, and coupons containing adhered cells were carefully removed, rinsed three times in phosphate-

Table 2
Bacterial strains used for the evaluation of antifouling efficiency of coatings.

Strain	Temperature	Culture medium
Pseudoalteromonas atlantica DSM 6840	22 °C	Marine Broth 2216
Marinobacter nauticus DSM 6819	25 °C	Marine Broth 2216
Pseudomonas aeruginosa ATCC BAA-47 (PA01)	37 °C	LB medium

Note: The cultivation temperatures were selected based on the recommendations provided by the culture supplier.

buffered saline (PBS, pH 7.4), and transferred to a new 24-well microtiter plate for further evaluation.

2.5.2. Assessment of biofilm formation

In this study, the formation of biofilm on metal coupons covered by coatings was evaluated by crystal violet staining and the MTT assay. Crystal violet staining, a widely adopted technique for the quantification of bacterial biofilms, is based on the binding of crystal violet molecules to the peptidoglycan bilayer of bacteria and the negatively charged molecules within the extracellular matrix [21–23]. This method provides insight into the total biomass, irrespective of the cell count within the biofilm. To enhance the robustness of biofilm quantification, it is advised that crystal violet staining be complemented with the assessment of metabolic activity using MTT. The MTT assay relies on the reduction of monotetrazolium salt (MTT) to formazan by NAD(*P*)H-dependent oxidoreductases. The presented formazan forms coloured crystals, and their absorbance allows the quantification of cellular oxidoreductase activity [24–26]. As NAD(*P*)H-dependent oxidoreductases are localized on the cell membrane and within the mitochondria critical for cellular vitality (in eukaryotic cells), their activity indirectly reflects the viability of cells [27]. The combination of these two methodologies provides comprehensive insights into biofilm volume and the quantity of viable cells and, consequently, infers the extent of the extracellular matrix.

2.5.3. Total biomass determination

The determination of total biomass was processed according to Doll et al. [28]. Into each well-containing coupon with adhered bacteria were added 1000 μL of crystal violet (CV) solution (0.1 % (m/v), Penta, CZ,) and the plates were kept statically for 20 min for cell staining. Afterwards, the coupons were washed with saline (three times, 2000 μL). Subsequently, 1000 μL of ethanol (96 %, Penta, CZ) was added to the coupons and incubated statically for 10 min at room temperature. The homogenised aliquots of 100 μL were transferred to a 96-well plate (Gama Group, CZ) and analysed at 580 nm using a UV–Vis spectrophotometer Infinite M200 Pro Reader (Tecan, CH). The determination was carried out in 4 parallels in 3 biological replicates.

2.5.4. Metabolic activity determination

The metabolic activity was performed according to Kulišová et al. [25]. Into each well-containing coupon with adhered bacteria were added 600 μL of glucose solution (Penta, CZ, 57.4 g L^{-1} in PBS) and 500 μL of MTT solution (Acros Organics, USA, 1.0 g L^{-1} in PBS) and the plates were incubated on an orbital shaker for 1 h in a dark (150 rpm, optimal temperature for specific microorganism). After incubation, 1000 μL of solvent solution (pH 4.7) composed of 160 g L^{-1} SDS, 400 g L^{-1} DMF, and 20 g L^{-1} acetic acid, diluted in PBS was added to each well and the plate was again incubated for 30 min in the dark at 150 rpm. The homogenised aliquots of 100 μL were transferred to a 96-well plate (Gama Group, CZ) and analysed at 570 nm using a UV–Vis spectrophotometer Infinite M200 Pro Reader (Tecan, CH). The determination was carried out in 4 parallels in 3 biological replicates.

3. Results and discussion

3.1. Coating design

In this study, the weight ratio of the hydrophilic to the hydrophobic part of the coating was fixed at 2:8, which was determined based on preliminary experiments (**Fig. S1**) and theoretical analysis [29,30]. This combination provides a dual protection mechanism, in which the hydrophilic part can effectively attract water and form a protective film that prevents direct biological attachment, while the hydrophobic part is mainly responsible for repelling water, further reducing the possibility of biological adhesion [30]. By incorporating lignin into the coating, we not only take advantage of its natural antibacterial capabilities but also increase the durability and stability of the coating owning to lignin's anti-oxidant characteristics, making it more suitable for applications in harsh marine environments (Fig. 3). This study evaluates the impact of these factors on coating performance by comparing lignin from different sources (see section **Lignin structural analysis**). This approach not only helps to understand the specific contribution of different types of lignin to coating performance but also provides valuable data and experience for future coating design.

3.2. Lignin structural analysis

Initially, four lignins were screened as potential components for the anti-fouling coatings. Due to the reported importance of functionalities such as phenolic hydroxyl groups when evaluating properties such as antioxidant and antimicrobial activity [31], ^{31}P NMR was performed (Table 3). Regarding antimicrobial activity, the situation is more elaborate than the content of specific hydroxyl and oxygen functionalities and is action-site dependent. Meanwhile, an amphiphilic character is in general considered important [32]. In this sense the acid extracted lignins (BA and SA) display interesting properties where their elevated total OH (phenolic OH content; 4.02 and 4.40 mmol/g, respectively) is somewhat disproportionate to what one would expect from depolymerized (through hydrolysis) aryl-ethers when considering the aliphatic OH content. Instead, and because of the significant content of condensed OH in the isolated spruce lignins, this is indicative of side-chain oxidation and 5-coupling of the guaiacyl units as suggested previously [33,34]. Introducing such changes during the lignin extraction process would retain the amphiphilic nature of the isolates and instead enrich the content of oxygen with a higher oxidation state and the content of aromatic carbons. Related to the solubilities of the various lignins in pure acetone (Fig. 4), this appears to promote the associated dissolution where not the overall OH content promotes solubility, but instead increased contents of condensed OH (and total phenolic OH) alongside a low aliphatic OH content. However, other properties such as the lignin molecular weight will also influence this and make the overall picture more complex.

As the coating synthesis protocol involves the application of polymer dissolution in pure acetone, solubility of the lignin as high as possible is desirable to avoid large structural heterogeneities. Because both acid-extracted lignins present overall high solubilities in acetone (close to 100 %), these were thus chosen for further investigation. As recently elaborated [35], the ability of lignins to display close-to-complete dissolution in pure acetone appears largely related to their chemical characteristics. Herein, the chemistry partially mitigates from close-to-native (especially evident for BA as evident from the P-NMR data presented herein but also supported elsewhere [36]) to instead display partial traits of sulfuric acid lignins (as for BA and SA) with the simultaneous introduction of sugar dehydration products which promotes solubility in pure acetone. As highlighted in, and relevant for the lignins further investigated herein is their botanical origin being either hardwood or softwood, where the latter is more prone, due to its vacant 5-position, to form aromatic condensed structures. [35] This, alongside easier depolymerization upon acidic conditions for guaiacol-rich lignins, is considered to eventually yield an elevated acetone dissolution capacity when compared to SA to BA [36,37].

3.3. FTIR analysis

The FTIR-ATR characterization of BA lignin and BA-PU is shown in Fig. 5. The BA-PU of Fig. 5 shows that the characteristic peak between 2240 cm^{-1}-2260 cm^{-1} of the NCO belonging to isocyanates is not present [38]. This indicates that the NCO reaction was completed, and carbamate was successfully formed. At the same time, the addition of lignin did not cause significant changes. With the addition of BA lignin, two peaks corresponding to the –OH and –C=O– group shift (Fig. 5a**)** [39]. As the concentration of BA in the blend increases, the spectrum of

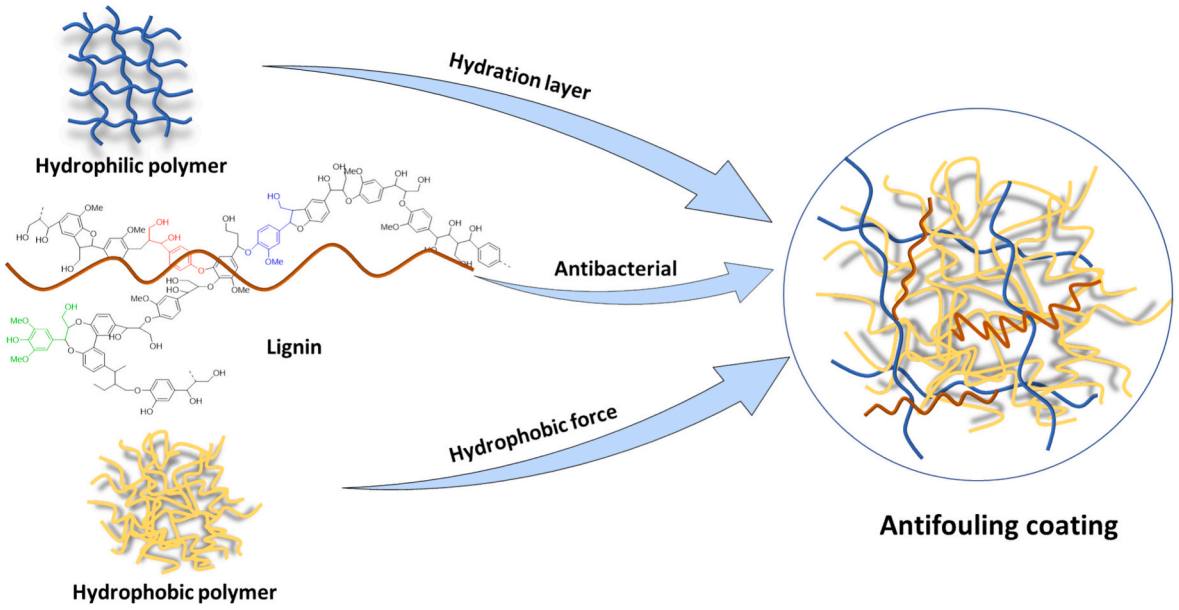

Fig. 3. Antifouling coating design strategy.

Table 3
Functional group characteristics (^{31}P NMR) of the various lignins.

Functional groups	BA [mmol/g]	B [mmol/g]	SA [mmol/g]	S [mmol/g]
Aliphatic OH	1.70	4.15	1.36	1.14
Condensed OH	2.88	1.42	1.83	1.55
G type OH	0.91	0.71	2.13	1.82
H type OH	0.23	0.13	0.43	0.41
Total Phenolic OH	4.02	2.26	4.40	3.78
Acidic OH	0.11	0.20	0.24	0.28

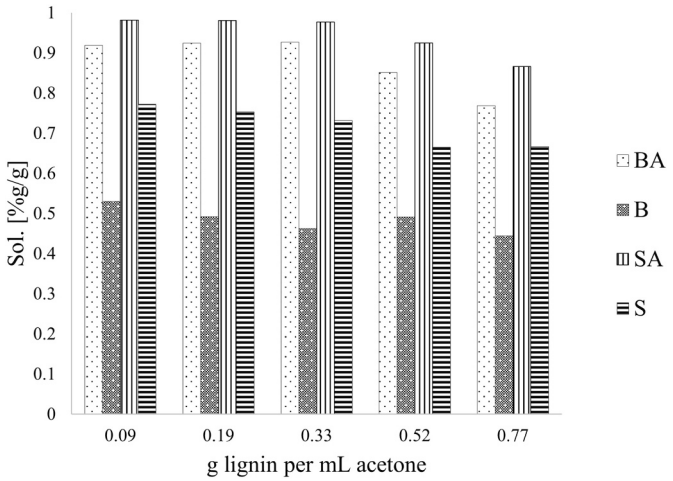

Fig. 4. Lignin solubility in pure acetone.

the hydroxyl region shows a red shift of the –OH group in PU from 3337 cm^{-1} to 3353 cm^{-1}(Fig. 5b), which is because of the —O— group in the lignin. [40] The –OH forms a hydrogen bond. At the same time, the peak of the –C=O– group in PU is blue-shifted. This was attributed to the formation of hydrogen bonds with the –OH groups in lignin [41] . The same results can be obtained from the FITR spectra of SA-PU **(Fig. S6).** These shifts indicate the formation of hydrogen bonds between lignin and PU, stabilizing the composite [42]. Lignin's hydroxyl and carbonyl groups interact with both hydrophilic and hydrophobic segments of PU, enhancing the coating's balance of properties essential for antifouling and wear resistance.

3.4. Thermal stability

Fig. 6**a** and **b** show the thermal stability analysis results for BA lignin and BA-PU. From Fig. 6**a,** 0 % Lignin-PU has two main areas of mass loss: 300 °C to 350 °C temperature range and 350 °C to 430 °C temperature range. This is mainly because 0 % Lignin-PU is composed of hydrophilic PU and hydrophobic PU (mass ratio 2:8), resulting in a residue of only 1.77 %. With the addition of BA lignin, the mass percentage of residues (char) is continuously increasing reaching up to 20 % for the 40 % BA-PU. From the derivative thermogravimetric (DTG) analysis (Fig. 6**b**), it can be found that when BA lignin is added at a small amount (10 %), there are three thermogravimetric peaks. As the lignin content increases, the thermogravimetric peaks gradually change to two, and the temperature of the occurrence of the thermogravimetric peak gradually decreases. This is because the interaction between a small amount of lignin and PU is not strong, and the pyrolysis processes of the three substances can be clearly distinguished. However, when the amount of lignin increases and the content exceeds the proportion of hydrophilic PU, the interaction between lignin and PU is enhanced, forming more hydrogen bonds. The two thermogravimetric peaks gradually overlap [43]. These results indicate that the thermal stability of BA-PU is enhanced with the incorporation of BA lignin. The presence of a heat-resistant lignin group in coatings enhances their ability to tolerate high temperatures, and eventually will extend the life and durability of the coating [44].

Differential scanning calorimetric measurements were carried out for BA-PU, and the resulting thermograms are presented in Fig. 6**c**. When lignin is incorporated into PU, the T_g starts to shift to higher temperatures. It increased from −33.2 °C to 41.7 °C. There are two reasons for this: (a) The lignin molecular chain and the PU molecular chain form hydrogen bonds. These hydrogen bonds hinder the movement of the coating's molecular chains, which require higher temperatures for them to move. (b) As the proportion of lignin in coatings continues to increase, a higher number of lignin molecules exist in the coating, making the movement of PU molecular chains more difficult. [45] A higher T_g means the coating becomes harder and stiffer at room temperature, thereby enhancing its durability and ability to withstand mechanical stress, wear and environmental conditions [46]. This change

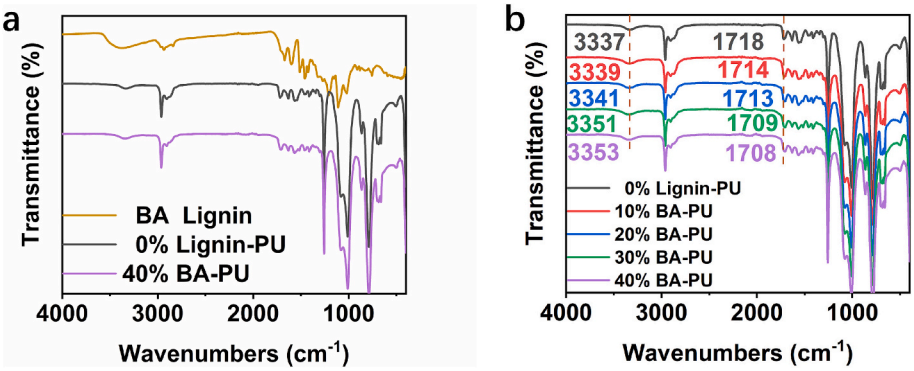

Fig. 5. a) FTIR-ATR spectra of BA lignin, 0 % Lignin-PU and 40 % BA-PU; b) FTIR- ATR spectra of BA-PU.

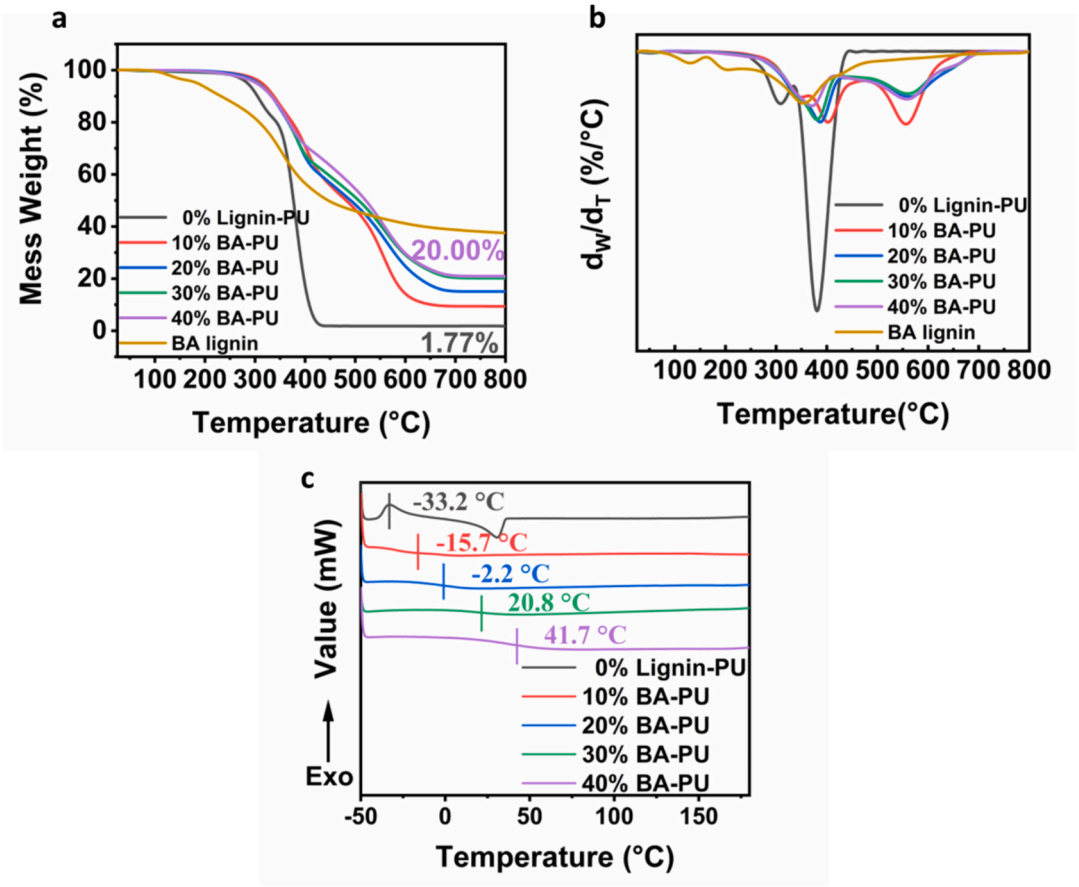

Fig. 6. a) and b) TG and DTG diagram of BA lignin, BA-PU, and c) DSC profiles of PU and BA lignin/PU blends.

is critical for ships as it ensures the coating retains its protective properties against water, UV radiation and corrosive elements and reduces maintenance requirements while improving fuel efficiency by minimizing drag. Overall, the shift to higher T_g represents a significant improvement in coating operating efficiency and longevity [47]. SA-PU also demonstrate similar results (**Fig. S7**).

3.5. Contact angle

The hydrophobicity of the control sample (uncoated steel sheet) and Lignin-PU composite membrane was evaluated by measuring the water contact angle. The results are shown in Fig. 7 and **Fig. S8**. As expected, the uncoated control sample shows a low water contact angle of 60°. For 0 % Lignin-PU, due to the presence of hydrophobic groups on the surface of the film, the film exhibits a higher water contact angle of 99°. After adding 10 % BA Lignin, the water contact angle is increased to 103.2°, which continuously increased upon increasing the BA content and reached a maximum of 114°. This means that the presence of hydrophobic lignin and its synergistic interaction with PU chains appears to result in a network barrier in the composite film, with a concomitant increase in the hydrophobicity of the film [48].

3.6. Anti-scratch

It can be seen in Fig. 8 that, under the action of the same vertical force, the embedding depth of the coating is also different with different lignin contents. Higher lignin content has a shallower embedment depth which means a better anti-scratch property. At the same time, it can also

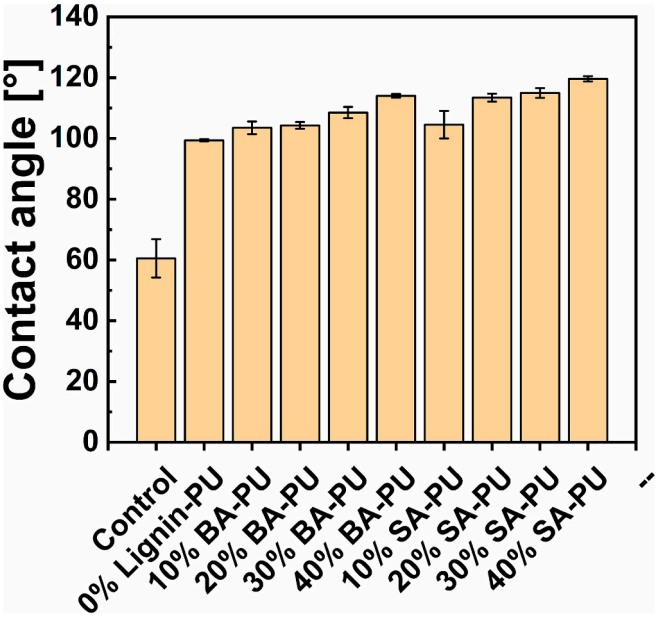

Fig. 7. The water contact angle of control sample, BA-PU and SA-PU.

be found (Fig. 8 and **Fig. S10**) that the increase in lignin content brings higher coating hardness and contact modulus. This shows that the addition of lignin improves the mechanical strength of the coating which contributes to the better anti-scratch properties. This is because lignin and PU molecular chains form dense and strong intermolecular hydrogen bonds, which is consistent with the results of previous FTIR and thermal stability.

3.7. Tribological performance test

The coefficient of friction of 0 % lignin-PU coating and BA-PU is displayed in Fig. 9. The friction coefficient decreases with increasing coating hardness, which indicates that the energy dissipation mechanism of PU is related to the viscoelastic deformation of the specimen and sliding in the boundary state [49]. The friction coefficient of PU coating is around 0.8, and the friction coefficient of 20 % BA-PU coating is reduced to 0.08. Boundary lubrication plays a major role in this system. In the process of increasing the lignin content from 0 % to 30 %, the addition of lignin increases the mechanical strength of the coating, forming a smooth and strong surface layer on the surface, thereby reducing the boundary friction on the surface. However, when the lignin content increases to 40 %, many lignin particles (caused by agglomeration) accumulate on the surface, increasing the surface roughness and thus increasing friction. The results obtained by SA-PU (**Fig. S11**) are the same. Lower friction coefficients can lead to decreased energy consumption and reduced wear, extending the lifespan of both the coating and the underlying material. Additionally, the smoother and stronger surface provided by optimal lignin content enhances the durability and performance of the coating, making it ideal for high-stress environments. Smoother coatings are also expected to prevent bacterial attachment.

3.8. Protein adsorption behavior

For the protein resistance behavior, the coatings with 30 % lignin were selected owning to their low friction while providing high abrasion resistance. The protein resistance of different coatings was measured by QCM-D (Fig. 10), which depicts the time dependence of the frequency change (Δf) of coating adsorption to bovine serum albumin on a reference surface. For the control sample (no coating applied), Δf decreased significantly after rinsing with BSA solution, indicating considerable

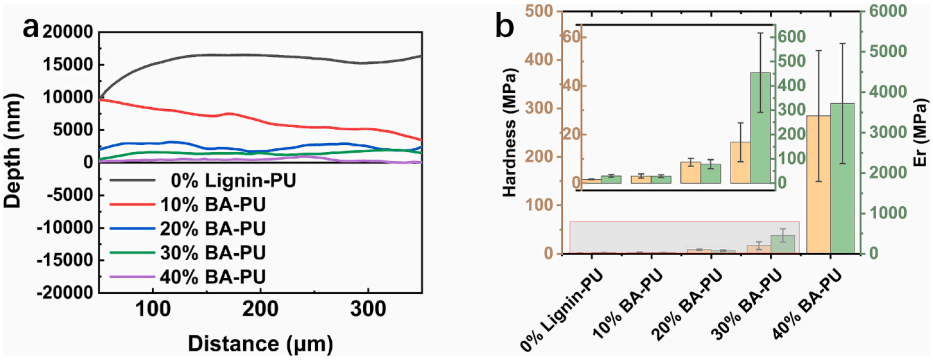

Fig. 8. a) the Nano scratch test of 0 % Lignin-PU and BA-PU; b) the hardness modulus and contact modulus of 0 % Lignin-PU and BA-PU.

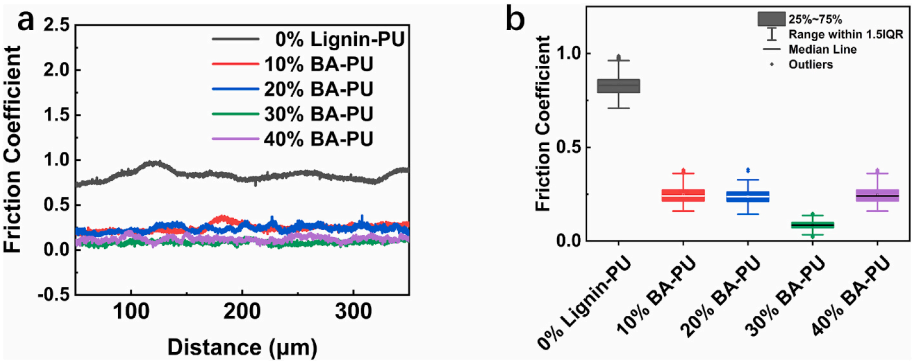

Fig. 9. The friction coefficient of 0 % Lignin-PU and BA-PU.

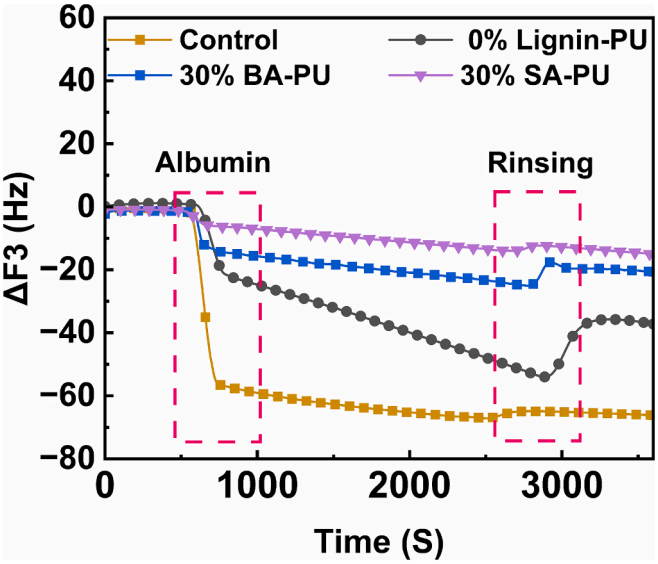

Fig. 10. The QCM-D curves of the control sample, 0 % lignin-PU, 30 % BA-PU and 30 % SA-PU.

protein adsorption. For 0 % Lignin-PU, the change in Δf decreased slightly, indicating minor protein adsorption onto the coating surface [50]. With the addition of lignin, the coating becomes resistant to proteins. As mentioned above, the hydrophilic PU in the amphiphilic telomer can appear on the surface to form a hydration layer to resist protein adsorption effectively. At the same time, the addition of lignin in the physical form of a complex pair effectively regulates the surface of the coating surface. It can further reduce the adsorption of proteins, thereby achieving an anti-fouling effect.

3.9. Antibacterial activity

3.9.1. Evaluation of coating preparation

Prior to the evaluation of antifouling capacities, it was essential to establish a reproducible method for the application of the lignin coatings. Striking a balance between adequate coverage of the metal coupon and surface uniformity became essential, given that an increase in the coating amount correlated with increased thickness and roughness of the surface (Supplementary Information, Fig. **S12**). Surface changes have the potential for enhanced adhesion of microorganisms. To monitor the coating coverage, scanning electron microscopy (SEM) was employed, with penetration depths reaching around 9 μm under the applied voltage of 30 kV. [51] Elemental analysis (Supplementary Information, **Fig. S13**) revealed that a three-layer coating sufficiently covered the steel coupon. In contrast, the application of only two layers resulted in areas where elements characteristic of steel were evident in the energy-dispersive X-ray spectroscopy (EDS) images.

3.9.2. Assessment of biofilm formation

Three Gram-negative, rod-shaped bacterial strains with polar flagella were selected for the assessment of antifouling properties. The Gram-negative bacteria are recognized as the major primary colonizers and are predominantly present in marine biofilms [52–55]. The strains used in the study were *Pseudoalteromonas atlantica*, *Marinobacter nauticus* (synonyms: *Pseudomonas nautica*; *Marinobacter aquaeolei*; *Marinobacter hydrocarbonoclasticus*) [56], and *Pseudomonas aeruginosa*. Although the selected marine microorganisms, all belonging to the Gammaproteobacteria, were initially grouped together due to shared physiological traits resembling pseudomonas-like marine bacteria [57], contemporary classification has assigned them to distinct genera. Bacteria of the genus *Marinobacter* [58,59] and *Pseudoaltermonas* [60] are widely distributed and commonly detected in various marine environments including surface waters near the shores. *P. atlantica* is a recognized causative agent of biofilm formation in the marine milieu [61], similar to the genus *Marinobacter* [62]. As a control strain in this study, *P. aeruginosa* was chosen for its role as a model strain in biofilm research [63].

In general, *P. atlantica* exhibited the highest biofilm biomass production (Fig. 11), likely attributed to the genus' notable proficiency in extracellular polymeric substance (EPS) production [64]. Across the three tested strains, coatings incorporating SA lignin consistently demonstrated lower biofilm production compared to those containing BA lignin. Notably, for BA lignin, the highest total biomass (highest absorbance) was observed at a 20 % lignin content in the coating, beyond which a decline in biofilm biomass content ensued with escalating lignin concentrations. Conversely, the varying content of SA lignin in the coating did not exhibit a globally significant impact on biofilm biomass. A noteworthy observation pertains to the strain-specific variation in total biofilm biomass production between the control coating without lignin content and the lignin coatings. Specifically, in the case of *P. atlantica*, the control coating without lignin content showed similar amounts of biofilm biomass as coatings containing SA lignin. For *M. nauticus* and *P. aeruginosa* the control coating without lignin content showed the lowest total biomass values. Lignin-containing coatings (30 % and 40 % of both types of lignin) in comparison with commercially available coatings showed a better antifouling effect as evidenced by the diminished total biofilm biomass in all three strains tested.

In terms of metabolic activity among biofilm cells, *P. aeruginosa* generally exhibited the highest measured values (Fig. 12). Across the three tested strains, coatings incorporating SA lignin consistently demonstrated lower metabolic activity compared to those containing BA lignin, aligning with total biomass determination. Next, a similar trend is observable for all three tested strains, where increasing lignin content correlates with an increase in the metabolic activity of biofilm cells, although significant differences are only observable in *P. atlantica*. The determined values for the other two strains are very close within the determined deviation values. Similarly, as observed in the determination of total biofilm biomass, there is a strain-specific variation in metabolic activity between the control coating without lignin content and the lignin coatings. Specifically, in the case of *P. atlantica*, coatings with lignin content revealed a reduction in metabolic activity in comparison with the control coating without lignin, while an inverse trend was observed for *M. nauticus* and *P. aeruginosa*. Lignin-containing coatings in comparison with commercially available coating Commercial 1 showed a better antifouling effect as evidenced by the diminished metabolic activity in all three strains tested. The coating Commercial 2 (active ingredient Cu_2O) was excluded from the evaluation due to its unwanted side interaction with tetrazolium salt.

The process of bacterial adhesion relies predominantly on physicochemical interactions between the bacterial surface and the substrate [65]. Surface structures like flagella or pili play a pivotal role in primary bacterial adhesion [66]. The antifouling efficacy of coatings is a connection of various properties, encompassing hydrophobicity, zeta potential, and structural characteristics such as substrate roughness, texture, material porosity and fibrousness [67–69]. The coating's resistance to bacterial adhesion and biofilm propagation can be enhanced by incorporating substances with antimicrobial properties [70]. In our study, as the lignin concentration increased in the coating, we anticipate alterations in structural characteristics, which could possibly augment surface area for bacterial adhesion and increase hydrophobicity (supported by contact angle measurement – Fig. 7). Simultaneously, higher concentrations of lignin suggest the potential of enhancing non-specific antimicrobial effects [71]. The presence of antimicrobial properties in the lignin within the coating indirectly implies a superior efficacy of coating containing SA lignin compared to BA lignin. This can be ascribed to the different content of total phenolic hydroxyl groups, which is higher in SA lignin (Table 3 – Structural motives of lignins). Lignin

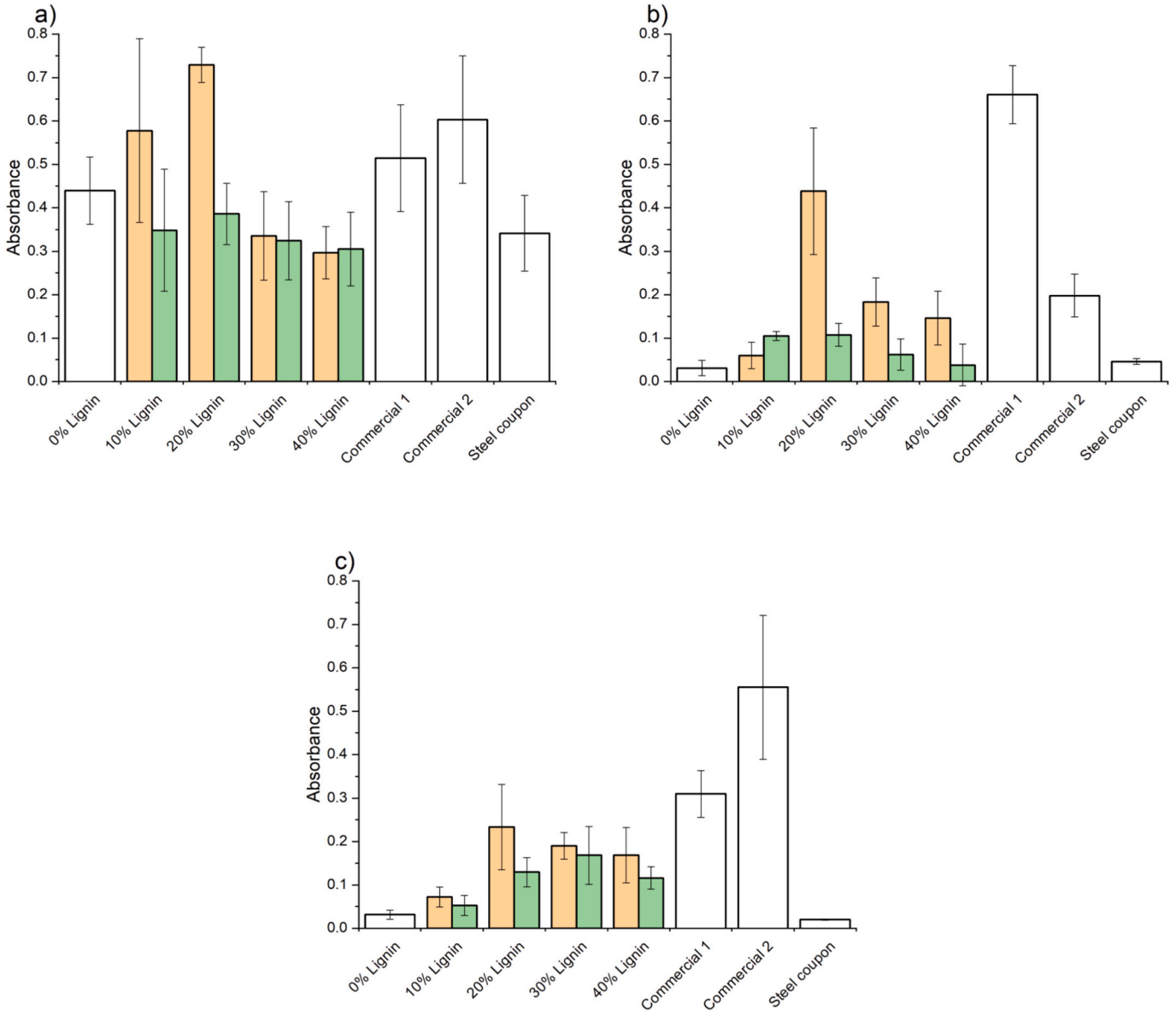

Fig. 11. Total biomass of adhered cells a) *Pseudoalteromonas atlantica*; b) *Marinobacter nauticus*; c) *Pseudomonas aeruginosa* on metal coupons coated with the developed coatings containing BA lignin; SA lignin and commercial coatings Commercial 1 (biocide-free coating); Commercial 2 (active compound Cu_2O).

generates reactive oxygen species and destabilizes bacterial membranes, which contributes to its antibacterial effects [72,73]. Mentioned hydroxyl phenols are recognized as one of the main motives responsible for this action [74]. For example, phenolate ions can promote the formation of hydroxyl radicals [75], leading to membrane lipid peroxidation [76]. Furthermore, the complex polyphenol structure of lignin makes it difficult for bacteria to develop resistance due to its non-specific effects [77]. Despite the benefit of increased antimicrobial activity when exposed to a high concentration of bacteria within a short time frame, the paramount importance probably lies in the physical properties of the coatings. This is indicated by findings for *P. aeruginosa* and *M. nauticus*, which showed lower biomass and metabolic activity on a smooth coating without lignin compared to coatings with lignin content. The hypothesis that changes in surface characteristics of our studied coatings may facilitate the rapid adhesion of bacteria aligns with Friedlander et al., who demonstrated that flagellated *E. coli* adheres more effectively to rough surfaces [78]. Simultaneously, the increased hydrophobicity of lignin coatings in comparison to the coating without lignin could support the flagellum's affinity for the studied bacteria, a phenomenon observed in the case of *P. aeruginosa* (PA01) in the study conducted by Bruzaud et al. [79].

The contrasting behavior observed in *P. atlantica*, which easily colonized lignin-free coating, can be linked to its extracellular polymeric substances (EPS) production, that is described as a good flocculating and sticky agent with a very high ability to adhere to available surfaces [80]. Specifically, transparent-exopolymer particles (TEP) produced by *P. atlantica* participate in marine gel particle (MGP) formation [81,82]. Due to their aggregation properties these particles play a role in establishing a conditioning layer conducive to the adhesion of bacteria and facilitating the formation of biofouling [83]. On the contrary, Ennouri et al. noted in their work related to *Marinobacter hydrocarbonoclasticus* biofilm sparse extracellular material resembling webs and thin fibers [84]. The robust production of EPS by *P. atlantica* probably explains the strain-specific variations observed in total biomass and metabolic activity compared to other tested strains. The substantial impact of EPS production in *P. atlantica* is further suggested by comparing the data with the biofilm-forming control, *P. aeruginosa*. In general, *P. aeruginosa* exhibited a lower signal in total biomass determination but a higher

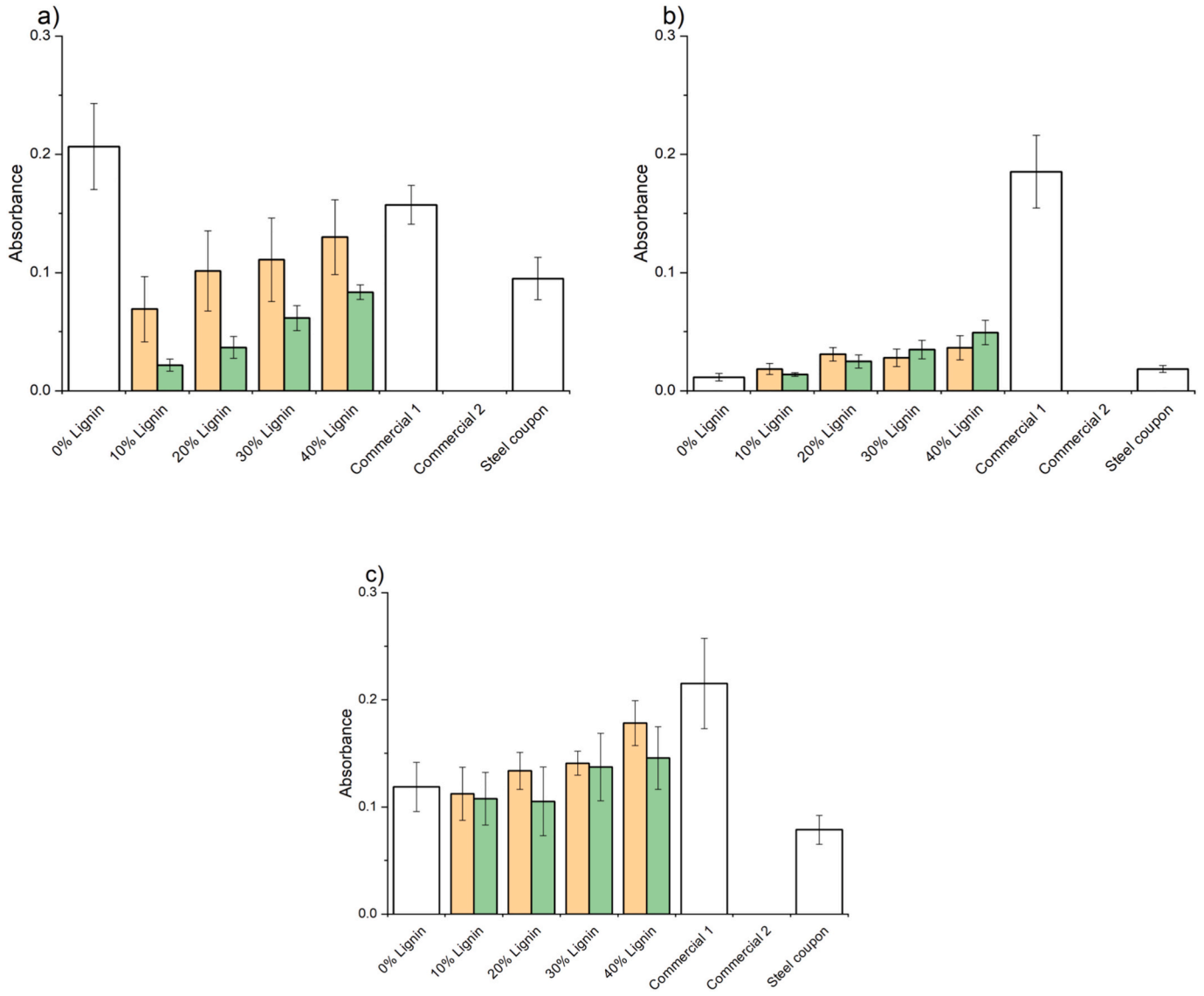

Fig. 12. Metabolic activity of adhered cells a) *Pseudoalteromonas atlantica*; b) *Marinobacter nauticus*; c) *Pseudomonas aeruginosa* on metal coupons coated with the developed coatings containing BA lignin; SA lignin and commercial coatings Commercial 1 (biocide-free coating). Commercial 2 was excluded from the study due to interaction with tetrazolium salt.

signal in metabolic activity determination, contrasting with the behavior observed in *P. atlantica*. The increasing metabolic activity observed in *P. atlantica* with the rising concentration of lignin within the coating may be attributed to the strain's extensive degradation potential [71]. This hypothesis supports findings from Lu et al., affirming the *Pseudoalteromonas* genus's capability to degrade compounds derived from lignin [85]. On the contrary, our results suggest that lignin's complex structure poses a challenge for *M. nauticus*, a member of the versatile genus *Marinobacter*, in colonizing and degrading efficiently our coatings [86,87].

Lignin-containing coatings outperformed commercial coatings in biofilm suppression of both model marine bacteria and the biofilm-model strain *P. aeruginosa* as evidenced by lower total biomass and metabolic activity compared to Commercial 1 and Commercial 2. The considerable colonization of commercial coatings by *P. atlantica* is likely attributed to the EPS described earlier. Commercial 2 containing Cu_2O as an active compound may have had its effects suppressed by the presence of negatively charged EPS, capable of binding positively charged metal ions [80,88]. Moreover, representatives of the genus *Pseudoalteromonas*, as shown by Zan et al., respond to copper exposition by forming biofilms, which agrees with high signal in biomass determination in the case of Commercial 2 [89]. Strains of the genus *Marinobacter* possess the genes involved in heavy metal resistance which probably allowed *M. nauticus* colonization despite the presence of Cu_2O in Commercial 2 [87]. The significant increase in total biomass and metabolic activity of *M. nauticus* on Commercial 1, which consists of a mixture of petroleum substances, is probably the result of the ability of this genus to produce a substantial quantity of bioemulsifiers (biosurfactants), likely facilitating bacterial adhesion to hydrophobic surfaces and the breakdown of water-immiscible materials [62,90,91]. Furthermore, the strains of genus *Marinobacter* have the capacity to degrade various hydrocarbons, often linked to oil spills and form oleolytic biofilms at the interface of water with carbon, whether in liquid or solid form [58,84].

4. Conclusions

This study successfully developed a new type of marine antifouling coating based on lignin, which shows excellent antifouling properties with minimized impact on the environment. Specifically, applying

lignin in the coating increased the water contact angle by 14.5 %, indicating improved surface hydrophobicity. Moreover, the mechanical strength of the coating was enhanced by approximately 200 %, significantly boosting its durability in harsh marine environments. Additionally, the friction coefficient was reduced by about 85 %, further contributing to its efficiency in preventing organism adhesion. These improvements underscore the feasibility of using natural renewable resources like lignin to develop environmentally friendly marine engineering materials. Notably, coatings with lignin not only provide an increase in surface hydrophobicity but also enhance antimicrobial activity. This achievement not only provides a new material choice for marine engineering but also lays a solid foundation for the future protection of the marine environment. To advance lignin-based coatings, future research should focus on optimizing lignin extraction processes to enhance yield and purity, exploring various lignin composites to improve mechanical, thermal, and antifouling properties, evaluating long-term environmental impacts in real-world marine settings, and developing scalable, cost-effective production methods to facilitate commercial adoption.

CRediT authorship contribution statement

Zhipeng Wu: Writing – review & editing, Writing – original draft, Methodology, Formal analysis, Data curation, Conceptualization. **Petter Paulsen Thoresen:** Writing – original draft, Methodology, Formal analysis, Data curation. **Dominik Maršík:** Writing – original draft, Methodology, Formal analysis, Data curation. **Leonidas Matsakas:** Writing – original draft, Methodology, Formal analysis, Data curation. **Markéta Kulišová:** Writing – original draft, Methodology. **Karel Fous:** Methodology, Formal analysis, Data curation. **Olga Maťátková:** Investigation, Formal analysis, Data curation. **Jan Masák:** Writing – original draft, Methodology, Formal analysis, Data curation. **Ulrika Rova:** Methodology, Data curation. **Erik Ytreberg:** Writing – original draft, Methodology, Formal analysis, Data curation. **Lena Granhag:** Writing – original draft, Formal analysis, Data curation. **Paul Christakopoulos:** Supervision, Methodology, Formal analysis, Data curation, Conceptualization. **Yijun Shi:** Writing – review & editing, Writing – original draft, Supervision, Methodology, Funding acquisition, Formal analysis, Data curation, Conceptualization.

Declaration of competing interest

The authors declare that they have no known competing financial interests or personal relationships that could have appeared to influence the work reported in this paper.

Acknowledgements

The authors thank the financial support from the Swedish Research Council for Environment, Agricultural Sciences and Spatial Planning (Formas, Project No. 2020-01258 and 2022-01047).

Appendix A. Supplementary data

Supplementary data to this article can be found online at https://doi.org/10.1016/j.ijbiomac.2024.137456.

Data availability

Data will be made available on request.

References

[1] R. Deng, T. Shen, H. Chen, J. Lu, H.-C. Yang, W. Li, Slippery liquid-infused porous surfaces (SLIPSs): a perfect solution to both marine fouling and corrosion? J. Mater. Chem. A 8 (16) (2020) 7536–7547, https://doi.org/10.1039/d0ta02000a.

[2] R.L. Townsin, The ship hull fouling penalty, Biofouling 19 Suppl(sup1) (2003) 9–15. doi:https://doi.org/10.1080/0892701031000088535.

[3] Y. Gu, L. Yu, J. Mou, D. Wu, M. Xu, P. Zhou, Y. Ren, Research strategies to develop environmentally friendly marine antifouling coatings, Mar. Drugs 18 (7) (2020) 371, https://doi.org/10.3390/md18070371.

[4] P.L. Cahill, L.W. Moodie, C. Hertzer, E. Pinori, H. Pavia, C. Hellio, M.A. Brimble, J. Svenson, Creating new Antifoulants using the tools and tactics of medicinal chemistry, Acc. Chem. Res. 57 (3) (2024) 2001–2011, https://doi.org/10.1021/acs.accounts.3c00733.

[5] C. Wei, G. Wang, M. Cridland, D.L. Olson, S. Liu, Corrosion Protection of Ships, Elsevier, Handbook of Environmental Degradation of Materials, 2018, pp. 533–557.

[6] S. Silver, T. Phung le, G. Silver, Silver as biocides in burn and wound dressings and bacterial resistance to silver compounds, J. Ind. Microbiol. Biotechnol. 33 (7) (2006) 627–634, https://doi.org/10.1007/s10295-006-0139-7.

[7] D. Claisse, C. Alzieu, Copper contamination as a result of antifouling paint regulations? Mar. Pollut. Bull. 26 (7) (1993) 395–397, https://doi.org/10.1016/0025-326X(93)90188-P.

[8] M.R.L. Jones, P.M. Ross, Recovery of the New Zealand muricid dogwhelk Haustrum scobina from TBT-induced imposex, Mar. Pollut. Bull. 126 (2018) 396–401, https://doi.org/10.1016/j.marpolbul.2017.11.034.

[9] S. Magalhaes, L. Alves, B. Medronho, A.C. Fonseca, A. Romano, J.F.J. Coelho, M. Norgren, Brief overview on bio-based adhesives and sealants, Polymers (Basel) 11 (10) (2019) 1685, https://doi.org/10.3390/polym11101685.

[10] S.D. Kayode-Afolayan, E.F. Ahuekwe, O.C. Nwinyi, Impacts of pharmaceutical effluents on aquatic ecosystems, Sci Afr 17 (2022) e01288, https://doi.org/10.1016/j.sciaf.2022.e01288.

[11] M.K. Chug, E.J. Brisbois, Recent developments in multifunctional antimicrobial surfaces and applications toward advanced nitric oxide-based biomaterials, ACS Mater Au 2 (5) (2022) 525–551, https://doi.org/10.1021/acsmaterialsau.2c00040.

[12] M.M. Sreejaya, R.J. Sankar, K. Ramanunni, N.P. Pillai, K. Ramkumar, P. Anuvinda, V.S. Meenakshi, S. Sadanandan, Lignin-based organic coatings and their applications: a review, Mater Today-Proc 60 (2022) 494–501, https://doi.org/10.1016/j.matpr.2022.01.325.

[13] D. Kai, M.J. Tan, P.L. Chee, Y.K. Chua, Y.L. Yap, X.J. Loh, Towards lignin-based functional materials in a sustainable world, Green Chem. 18 (5) (2016) 1175–1200, https://doi.org/10.1039/c5gc02616d.

[14] S.K. Kyei, G. Darko, O. Akaranta, Chemistry and application of emerging ecofriendly antifouling paints: a review, J. Coat. Technol. Res. 17 (2) (2020) 315–332, https://doi.org/10.1007/s11998-019-00294-3.

[15] D.S. Bajwa, G. Pourhashem, A.H. Ullah, S.G. Bajwa, A concise review of current lignin production, applications, products and their environmental impact, Ind. Crop. Prod. 139 (2019) 111526, https://doi.org/10.1016/j.indcrop.2019.111526.

[16] E. Lizundia, M.H. Sipponen, L.G. Greca, M. Balakshin, B.L. Tardy, O.J. Rojas, D. Puglia, Multifunctional lignin-based nanocomposites and nanohybrids, Green Chem. 23 (18) (2021) 6698–6760, https://doi.org/10.1039/d1gc01684a.

[17] D. Wang, J. Zhao, P. Claesson, P. Christakopoulos, U. Rova, L. Matsakas, E. Ytreberg, L. Granhag, F. Zhang, J. Pan, Y. Shi, A strong enhancement of corrosion and wear resistance of polyurethane-based coating by chemically grafting of organosolv lignin, Materials Today Chemistry 35 (2024) 101833, https://doi.org/10.1016/j.mtchem.2023.101833.

[18] A. Granata, D.S. Argyropoulos, 2-Chloro-4,4,5,5-Tetramethyl-1,3,2-Dioxaphospholane, a reagent for the accurate determination of the uncondensed and condensed phenolic moieties in Lignins, J. Agric. Food Chem. 43 (6) (1995) 1538–1544, https://doi.org/10.1021/jf00054a023.

[19] Z.H. Jiang, D.S. Argyropoulos, A. Granata, Correlation analysis of 31P NMR chemical shifts with substituent effects of phenols, Magn. Reson. Chem. 33 (5) (1995) 375–382, https://doi.org/10.1002/mrc.1260330509.

[20] X. Meng, C. Crestini, H. Ben, N. Hao, Y. Pu, A.J. Ragauskas, D.S. Argyropoulos, Determination of hydroxyl groups in biorefinery resources via quantitative (31)P NMR spectroscopy, Nat. Protoc. 14 (9) (2019) 2627–2647, https://doi.org/10.1038/s41596-019-0191-1.

[21] C.I. Amador, R.O. Stannius, H.L. Roder, M. Burmolle, High-throughput screening alternative to crystal violet biofilm assay combining fluorescence quantification and imaging, J. Microbiol. Methods 190 (2021) 106343, https://doi.org/10.1016/j.mimet.2021.106343.

[22] G. Budin, H.J. Chung, H. Lee, R. Weissleder, A magnetic Gram stain for bacterial detection, Angew. Chem. Int. Ed. Eng. 51 (31) (2012) 7752–7755, https://doi.org/10.1002/anie.201202982.

[23] A. Popescu, R.J. Doyle, The Gram stain after more than a century, Biotech. Histochem. 71 (3) (1996) 145–151, https://doi.org/10.3109/10520299609117151.

[24] J. Gabrielson, M. Hart, A. Jarelov, I. Kuhn, D. McKenzie, R. Mollby, Evaluation of redox indicators and the use of digital scanners and spectrophotometer for quantification of microbial growth in microplates, J. Microbiol. Methods 50 (1) (2002) 63–73, https://doi.org/10.1016/s0167-7012(02)00011-8.

[25] M. Kulišová, O. Maťátková, T. Brányik, J. Zelenka, L. Drábová, I.J. Kolouchová, Detection of microscopic filamentous fungal biofilms–choosing the suitable methodology, J. Microbiol. Methods 205 (2023) 106676, https://doi.org/10.1016/j.mimet.2023.106676.

[26] T. Mosmann, Rapid colorimetric assay for cellular growth and survival: application to proliferation and cytotoxicity assays, J. Immunol. Methods 65 (1–2) (1983) 55–63, https://doi.org/10.1016/0022-1759(83)90303-4.

[27] M.V. Berridge, P.M. Herst, A.S. Tan, Tetrazolium dyes as tools in cell biology: new insights into their cellular reduction, Biotechnol. Annu. Rev. 11 (2005) 127–152 (https://).
[28] A. Doll, B.K. Holzel, S. Mulej Bratec, C.C. Boucard, X. Xie, A.M. Wohlschlager, C. Sorg, Mindful attention to breath regulates emotions via increased amygdala-prefrontal cortex connectivity, Neuroimage 134 (2016) 305–313, https://doi.org/10.1016/j.neuroimage.2016.03.041.
[29] K.P. Wang, D.Y. Hou, J. Wang, Z.X. Wang, B.H. Tian, P. Liang, Hydrophilic surface coating on hydrophobic PTFE membrane for robust anti-oil-fouling membrane distillation, Appl. Surf. Sci. 450 (2018) 57–65, https://doi.org/10.1016/j.apsusc.2018.04.180.
[30] M. Barletta, C. Aversa, E. Pizzi, M. Puopolo, S. Vesco, Design, manufacturing and testing of anti-fouling/foul-release (AF/FR) amphiphilic coatings, Prog. Org. Coat. 123 (2018) 267–281, https://doi.org/10.1016/j.porgcoat.2018.07.016.
[31] Y. Li, Y. Miao, L. Yang, Y. Zhao, K. Wu, Z. Lu, Z. Hu, J. Guo, Recent advances in the development and antimicrobial applications of metal-phenolic networks, Adv Sci (Weinh) 9 (27) (2022) e2202684, https://doi.org/10.1002/advs.202202684.
[32] A. Lobiuc, N.E. Paval, R. Mangalagiu II, G.C. Gheorghita, D. Teliban, V. Stoleru Amariucai-Mantu, Future antimicrobials: natural and functionalized Phenolics, Molecules 28 (3) (2023) 1114, https://doi.org/10.3390/molecules28031114.
[33] F.H.B. Sosa, A. Bjelic, J.A.P. Coutinho, M.C. Costa, B. Likozar, E. Jasiukaityte-Grojzdek, M. Grilc, A.M.D. Lopes, Conversion of Organosolv and Kraft lignins into value-added compounds assisted by an acidic deep eutectic solvent, Sustain Energ Fuels 6 (20) (2022) 4800–4815, https://doi.org/10.1039/d2se00859a.
[34] P.P. Thoresen, J. Hedlund, H. Lange, J. Hertzog, V. Carré, M. Zhou, A. Trubetskaya, F. Aubriet, J. Hedlund, T. Gustafsson, U. Rova, P. Christakopoulos, L. Matsakas, On the understanding of bio-oil formation from the hydrothermal liquefaction of organosolv lignin isolated from softwood and hardwood sawdust, Sustain Energ Fuels 7 (22) (2023) 5361–5373, https://doi.org/10.1039/d3se00976a.
[35] P. Paulsen Thoresen, Structure and Property Oriented Organosolv Lignin Extraction, Luleå University of Technology, 2024.
[36] P.P. Thoresen, I. Delgado Vellosillo, H. Lange, U. Rova, P. Christakopoulos, L. Matsakas, Furan distribution as a severity Indicator upon Organosolv fractionation of hardwood sawdust through a novel ternary solvent system, ACS Sustain. Chem. Eng. 12 (4) (2024) 1666–1680, https://doi.org/10.1021/acssuschemeng.3c07236.
[37] H. Yang, C.G. Yoo, X. Meng, Y. Pu, W. Muchero, G.A. Tuskan, T.J. Tschaplinski, A. J. Ragauskas, L. Yao, Structural changes of lignins in natural Populus variants during different pretreatments, Bioresour. Technol. 295 (2020) 122240, https://doi.org/10.1016/j.biortech.2019.122240.
[38] Z.H. Shen, J.L. Chen, G.F. Li, G. Situ, X.F. Ma, Y. Sha, D. Zhao, Q. Gu, M. Zhang, Y. L. Luo, Z.Y. Luo, Mechanically robust self-repairing polyurea elastomers: the roles of hard segment content and ordered/disordered hydrogen-bonding arrays, Eur. Polym. J. 181 (2022), https://doi.org/10.1016/j.eurpolymj.2022.111657.
[39] J.F. Kadla, S. Kubo, Lignin-based polymer blends: analysis of intermolecular interactions in lignin-synthetic polymer blends, Compos Part a-Appl S 35 (3) (2004) 395–400, https://doi.org/10.1016/j.compositesa.2003.09.019.
[40] P.C. Rodrigues, M.P. Cantao, P. Janissek, P.C.N. Scarpa, A.L. Mathias, L.P. Ramos, M.A.B. Gomes, Polyaniline/lignin blends: FTIR, MEV and electrochemical characterization, Eur. Polym. J. 38 (11) (2002) 2213–2217, https://doi.org/10.1016/S0014-3057(02)00114-3.
[41] D. Kun, B. Pukánszky, Polymer/lignin blends: interactions, properties, applications, Eur. Polym. J. 93 (2017) 618–641, https://doi.org/10.1016/j.eurpolymj.2017.04.035.
[42] G.C. Qi, W.J. Yang, D. Puglia, H.G. Wang, P.W. Xu, W.F. Dong, T. Zheng, P.M. Ma, Hydrophobic, UV resistant and dielectric polyurethane-nanolignin composites with good reprocessability, Mater Design 196 (2020) 109150, https://doi.org/10.1016/j.matdes.2020.109150.
[43] G.H. Xu, S.X. Ren, D. Wang, L. Su, G.Z. Fang, Fabrication and properties of alkaline lignin/poly (vinyl alcohol) blend membranes, Bioresources 8 (2) (2013) 2510–2520. https://ncsu.edu/bioresources/BioRes_08/BioRes_08_2_2510_Xu_RWSF_Fabr_Prop_Alk_Lignin_PVOH_Membranes_3735.pdf.
[44] C.I. Idumah, C.M. Obele, E.O. Emmanuel, A. Hassan, Recently emerging Nanotechnological advancements in polymer nanocomposite coatings for anti-corrosion, Anti-fouling and Self-healing, Surf Interfaces 21 (2020) 100734, https://doi.org/10.1016/j.surfin.2020.100734.
[45] S. Kubo, J.F. Kadla, Poly(ethylene oxide)/organosolv lignin blends: relationship between thermal properties, chemical structure, and blend behavior, Macromolecules 37 (18) (2004) 6904–6911, https://doi.org/10.1021/ma0490552.
[46] A. Roy, L.W. Mu, Y.J. Shi, Tribological properties of polyimide coating filled with carbon nanotube at elevated temperatures, Polym. Compos. 41 (7) (2020) 2652–2661, https://doi.org/10.1002/pc.25564.
[47] D.E. Curtin, R.D. Lousenberg, T.J. Henry, P.C. Tangeman, M.E. Tisack, Advanced materials for improved PEMFC performance and life, J. Power Sources 131 (1–2) (2004) 41–48, https://doi.org/10.1016/j.jpowsour.2004.01.023.
[48] R. Tian, Y. Liu, C. Wang, W. Jiang, S. Janaswamy, G. Yang, X. Ji, G. Lyu, Strong, UV-blocking, and hydrophobic PVA composite films containing tunable lignin nanoparticles, Ind crop, Prod 208 (2024) 117842, https://doi.org/10.1016/j.indcrop.2023.117842.
[49] D. Wang, J. Zhao, P. Claesson, P. Christakopoulos, U. Rova, L. Matsakas, E. Ytreberg, L. Granhag, F. Zhang, J. Pan, A strong enhancement of corrosion and wear resistance of polyurethane-based coating by chemically grafting of organosolv lignin, Materials Today Chemistry 35 (2024) 101833, https://doi.org/10.1016/j.mtchem.2023.101833.
[50] M. Wang, Q.Y. Xie, J.S. Pan, C.F. Ma, G.Z. Zhang, Strong yet tough cross-linked oligosiloxane elastomer with impact-resistant and antifouling properties, Chem. Eng. J. 464 (2023), https://doi.org/10.1016/j.cej.2023.142769.
[51] L.T. Gibson, ARCHAEOMETRY AND ANTIQUE ANALYSIS | metallic and ceramic objects, in: P. Worsfold, A. Townshend, C. Poole (Eds.), Encyclopedia of Analytical Science, Elsevier, Oxford, 2005, pp. 117–123.
[52] Z.Z. Jeliani, I. Sourinejad, M. Afrand, A. Shahdadi, M. Yousefzadi, Molecular identification of biofilm-forming marine bacterial strains isolated from different substrates of mangrove habitat, Iranian Journal of Science and Technology Transaction a-Science 46 (6) (2022) 1563–1574, https://doi.org/10.1007/s40995-022-01383-6.
[53] J. Antunes, P. Leao, V. Vasconcelos, Marine biofilms: diversity of communities and of chemical cues, Environ. Microbiol. Rep. 11 (3) (2019) 287–305, https://doi.org/10.1111/1758-2229.12694.
[54] N. Bernbom, Y.Y. Ng, S.M. Olsen, L. Gram, Pseudoalteromonas spp. serve as initial bacterial attractants in mesocosms of coastal waters but have subsequent antifouling capacity in mesocosms and when embedded in paint, Appl. Environ. Microbiol. 79 (22) (2013) 6885–6893, https://doi.org/10.1128/AEM.01987-13.
[55] H. Dang, C.R. Lovell, Bacterial primary colonization and early succession on surfaces in marine waters as determined by amplified rRNA gene restriction analysis and sequence analysis of 16S rRNA genes, Appl. Environ. Microbiol. 66 (2) (2000) 467–475, https://doi.org/10.1128/AEM.66.2.467-475.2000.
[56] B.J. Tindall, Marinobacter nauticus (Baumann et al. 1972) comb. nov. arising from instances of synonymy and the incorrect interpretation of the International Code of Nomenclature of Prokaryotes, Arch Microbiol 202(3) (2020) 657–663. doi:https://doi.org/10.1007/s00203-019-01761-6.
[57] J. Lee, D. Gibson, J.M. Shewan, A numerical taxonomic study of some Pseudomonas-like marine bacteria, Microbiology 98 (2) (1977) 439–451, https://doi.org/10.1099/00221287-98-2-439.
[58] P. Bonin, C. Vieira, R. Grimaud, C. Militon, P. Cuny, O. Lima, S. Guasco, C. P. Brussaard, V. Michotey, Substrates specialization in lipid compounds and hydrocarbons of Marinobacter genus, Environ. Sci. Pollut. Res. Int. 22 (20) (2015) 15347–15359, https://doi.org/10.1007/s11356-014-4009-y.
[59] J.Z. Kaye, J.B. Sylvan, K.J. Edwards, J.A. Baross, Halomonas and Marinobacter ecotypes from hydrothermal vent, subseafloor and deep-sea environments, FEMS Microbiol. Ecol. 75 (1) (2011) 123–133, https://doi.org/10.1111/j.1574-6941.2010.00984.x.
[60] K. Zheng, Y. Dong, Y. Liang, Y. Liu, X. Zhang, W. Zhang, Z. Wang, H. Shao, Y. Y. Sung, W.J. Mok, Genomic diversity and ecological distribution of marine Pseudoalteromonas phages, Marine life science & technology 5 (2) (2023) 271–285, https://doi.org/10.1007/s42995-022-00160-z.
[61] J.S. Wang, L.H. Peng, X.P. Guo, A. Yoshida, K. Osatomi, Y.F. Li, J.L. Yang, X. Liang, Complete genome of ECSMB14104, a Gammaproteobacterium inducing mussel settlement, Mar. Genomics 46 (2019) 54–57, https://doi.org/10.1016/j.margen.2018.11.005.
[62] L.J. Bird, R.L. Mickol, B.J. Eddie, M. Thakur, M.D. Yates, S.M. Glaven, Marinobacter: a case study in bioelectrochemical chassis evaluation, Microb. Biotechnol. 16 (3) (2023) 494–506, https://doi.org/10.1111/1751-7915.14170.
[63] M. Musken, S. Di Fiore, U. Romling, S. Haussler, A 96-well-plate-based optical method for the quantitative and qualitative evaluation of Pseudomonas aeruginosa biofilm formation and its application to susceptibility testing, Nat. Protoc. 5 (8) (2010) 1460–1469, https://doi.org/10.1038/nprot.2010.110.
[64] C. Roca, M. Lehmann, C.A. Torres, S. Baptista, S.P. Gaudencio, F. Freitas, M.A. Reis, Exopolysaccharide production by a marine Pseudoalteromonas sp. strain isolated from Madeira Archipelago Ocean sediments, New Biotechnol. 33 (4) (2016) 460–466, https://doi.org/10.1016/j.nbt.2016.02.005.
[65] M.M. Santore, Interplay of physico-chemical and mechanical bacteria-surface interactions with transport processes controls early biofilm growth: a review, Adv. Colloid Interf. Sci. 304 (2022) 102665, https://doi.org/10.1016/j.cis.2022.102665.
[66] G.A. O'Toole, R. Kolter, Flagellar and twitching motility are necessary for Pseudomonas aeruginosa biofilm development, Mol. Microbiol. 30 (2) (1998) 295–304, https://doi.org/10.1046/j.1365-2958.1998.01062.x.
[67] S. Achinas, N. Charalampogiannis, G.J.W. Euverink, A brief recap of microbial adhesion and biofilms, Applied Sciences-Basel 9 (14) (2019) 2801, https://doi.org/10.3390/app9142801.
[68] J.K. Oh, Y. Yegin, F. Yang, M. Zhang, J. Li, S. Huang, S.V. Verkhoturov, E. A. Schweikert, K. Perez-Lewis, E.A. Scholar, T.M. Taylor, A. Castillo, L. Cisneros-Zevallos, Y. Min, M. Akbulut, The influence of surface chemistry on the kinetics and thermodynamics of bacterial adhesion, Sci Rep-Uk 8 (1) (2018) 17247, https://doi.org/10.1038/s41598-018-35343-1.
[69] J. Strejc, L. Kyselova, A. Cadkova, D. Matoulkova, T. Potocar, T. Branyik, Experimental adhesion of and to stainless steel compared with predictions from interaction models, Chem. Pap. 74 (1) (2020) 297–304, https://doi.org/10.1007/s11696-019-00880-0.
[70] H.-C. Flemming, Microbial Biofouling: Unsolved Problems, Insufficient Approaches, and Possible Solutions, 2011.
[71] A.G. Morena, T. Tzanov, Antibacterial lignin-based nanoparticles and their use in composite materials, Nanoscale Adv 4 (21) (2022) 4447–4469, https://doi.org/10.1039/d2na00423b.
[72] A.G. Morena, A. Bassegoda, M. Natan, G. Jacobi, E. Banin, T. Tzanov, Antibacterial properties and mechanisms of action of Sonoenzymatically synthesized lignin-based nanoparticles, ACS Appl. Mater. Interfaces 14 (33) (2022) 37270–37279, https://doi.org/10.1021/acsami.2c05443.
[73] W.J. Yang, E. Fortunati, D.Q. Gao, G.M. Balestra, G. Giovanale, X.Y. He, L. Torre, J. M. Kenny, D. Puglia, Valorization of acid isolated high yield lignin nanoparticles as

innovative antioxidant/antimicrobial organic materials, ACS Sustain. Chem. Eng. 6 (3) (2018) 3502–3514, https://doi.org/10.1021/acssuschemeng.7b03782.
[74] G.H. Wang, Y. Xia, B.K. Liang, W.J. Sui, C.L. Si, Successive ethanol-water fractionation of enzymatic hydrolysis lignin to concentrate its antimicrobial activity, J. Chem. Technol. Biotechnol. 93 (10) (2018) 2977–2987, https://doi.org/10.1002/jctb.5656.
[75] R. Castaneda-Arriaga, A. Perez-Gonzalez, M. Reina, J.R. Alvarez-Idaboy, A. Galano, Comprehensive investigation of the antioxidant and pro-oxidant effects of phenolic compounds: a double-edged sword in the context of oxidative stress? J. Phys. Chem. B 122 (23) (2018) 6198–6214, https://doi.org/10.1021/acs.jpcb.8b03500.
[76] H. Yin, L. Xu, N.A. Porter, Free radical lipid peroxidation: mechanisms and analysis, Chem. Rev. 111 (10) (2011) 5944–5972, https://doi.org/10.1021/cr200084z.
[77] S.S. Nassarawa, G.A. Nayik, S.D. Gupta, F.O. Areche, Y.D. Jagdale, M.J. Ansari, H. A. Hemeg, A. Al-Farga, S.S. Alotaibi, Chemical aspects of polyphenol-protein interactions and their antibacterial activity, Crit. Rev. Food Sci. Nutr. 63 (28) (2023) 9482–9505, https://doi.org/10.1080/10408398.2022.2067830.
[78] R.S. Friedlander, H. Vlamakis, P. Kim, M. Khan, R. Kolter, J. Aizenberg, Bacterial flagella explore microscale hummocks and hollows to increase adhesion, Proc. Natl. Acad. Sci. USA 110 (14) (2013) 5624–5629, https://doi.org/10.1073/pnas.1219662110.
[79] J. Bruzaud, J. Tarrade, A. Coudreuse, A. Canette, J.M. Herry, E. Taffin de Givenchy, T. Darmanin, F. Guittard, M. Guilbaud, M.N. Bellon-Fontaine, Flagella but not type IV pili are involved in the initial adhesion of Pseudomonas aeruginosa PAO1 to hydrophobic or superhydrophobic surfaces, Colloids Surf. B: Biointerfaces 131 (2015) 59–66, https://doi.org/10.1016/j.colsurfb.2015.04.036.
[80] G. Qin, L. Zhu, X. Chen, P.G. Wang, Y. Zhang, Structural characterization and ecological roles of a novel exopolysaccharide from the deep-sea psychrotolerant bacterium Pseudoalteromonas sp, SM9913, Microbiology (Reading) 153 (Pt 5) (2007) 1566–1572, https://doi.org/10.1099/mic.0.2006/003327-0.
[81] S. Li, H. Winters, S. Jeong, A.H. Emwas, S. Vigneswaran, G.L. Amy, Marine bacterial transparent exopolymer particles (TEP) and TEP precursors: characterization and RO fouling potential, Desalination 379 (2016) 68–74, https://doi.org/10.1016/j.desal.2015.10.005.
[82] S. Li, H. Winters, L.O. Villacorte, Y. Ekowati, A.H. Emwas, M.D. Kennedy, G. L. Amy, Compositional similarities and differences between transparent exopolymer particles (TEPs) from two marine bacteria and two marine algae: significance to surface biofouling, Mar. Chem. 174 (2015) 131–140, https://doi.org/10.1016/j.marchem.2015.06.009.
[83] A.S.M. Al-Wahaibi, R.C. Upstill-Goddard, J.G. Burgess, Isolation and staining reveal the presence of extracellular DNA in marine gel particles, Gels 9 (3) (2023) 251, https://doi.org/10.3390/gels9030251.
[84] H. Ennouri, P. d'Abzac, F. Hakil, P. Branchu, M. Naitali, A.M. Lomenech, R. Oueslati, J. Desbrieres, P. Sivadon, R. Grimaud, The extracellular matrix of the oleolytic biofilms of Marinobacter hydrocarbonoclasticus comprises cytoplasmic proteins and T2SS effectors that promote growth on hydrocarbons and lipids, Environ. Microbiol. 19 (1) (2017) 159–173, https://doi.org/10.1111/1462-2920.13547.
[85] P. Lu, W. Wang, G. Zhang, W. Li, A. Jiang, M. Cao, X. Zhang, K. Xing, X. Peng, B. Yuan, Z. Feng, Isolation and characterization marine bacteria capable of degrading lignin-derived compounds, PLoS One 15 (10) (2020) e0240187, https://doi.org/10.1371/journal.pone.0240187.
[86] S. Rughoft, N. Jehmlich, T. Gutierrez, S. Kleindienst, Comparative proteomics of Marinobacter sp, TT1 Reveals Corexit Impacts on Hydrocarbon Metabolism, Chemotactic Motility, and Biofilm Formation, Microorganisms 9 (1) (2020) 3, https://doi.org/10.3390/microorganisms9010003.
[87] E. Singer, E.A. Webb, W.C. Nelson, J.F. Heidelberg, N. Ivanova, A. Pati, K. J. Edwards, Genomic potential of Marinobacter aquaeolei, a biogeochemical "opportunitroph", Appl. Environ. Microbiol. 77 (8) (2011) 2763–2771, https://doi.org/10.1128/AEM.01866-10.
[88] Q.L. Qin, Y. Li, Y.J. Zhang, Z.M. Zhou, W.X. Zhang, X.L. Chen, X.Y. Zhang, B. C. Zhou, L. Wang, Y.Z. Zhang, Comparative genomics reveals a deep-sea sediment-adapted life style of Pseudoalteromonas sp. SM9913, ISME J. 5 (2) (2011) 274–284, https://doi.org/10.1038/ismej.2010.103.
[89] S. Zan, J. Lv, Z. Li, Y. Cai, Z. Wang, J. Wang, Genomic insights into Pseudoalteromonas sp, JSTW coping with petroleum-heavy metals combined pollution, J Basic Microbiol 61 (10) (2021) 947–957, https://doi.org/10.1002/jobm.202100156.
[90] B. Klein, V. Grossi, P. Bouriat, P. Goulas, R. Grimaud, Cytoplasmic wax ester accumulation during biofilm-driven substrate assimilation at the alkane–water interface by *Marinobacter hydrocarbonoclasticus* SP17, Res. Microbiol. 159(2) (2008) 137–44. doi:https://doi.org/10.1016/j.resmic.2007.11.013.
[91] K.M. Handley, J.R. Lloyd, Biogeochemical implications of the ubiquitous colonization of marine habitats and redox gradients by Marinobacter species, Front. Microbiol. 4 (2013) 136, https://doi.org/10.3389/fmicb.2013.00136.